Available online at www.sciencedirect.com
SCIENCE DIRECT®
Vision Research 45 (2005) 3323–3342
Vision Research
www.elsevier.com/locate/visres

# Computational adaptation model and its predictions for color induction of first and second orders

Hedva Spitzer *, Yuval Barkan

*Department of Biomedical Engineering, Faculty of Engineering, Tel-Aviv University, 69978 Tel-Aviv, Israel*

Received 3 December 2003; received in revised form 23 May 2005

**Abstract**

The appearance of a patch of color or its contrast depends not only on the stimulus itself but also on the surrounding stimuli (induction effects–simultaneous contrast). A comprehensive computational physiological model is presented to describe chromatic adaptation of the first (retinal) and second (cortical) orders, and to predict the different chromatic induction effects. We propose that the chromatic induction of the first order that yields perceived complementary colors can be predicted by retinal adaptation mechanisms, contrary to previous suggestions. The second order of the proposed adaptation mechanism succeeds to predict the automatic perceived inhibition or facilitation of the central contrast of a texture stimulus, depending on the surrounding contrast. Furthermore, contrary to other models, this model is able to also predict the effect of variegated surrounding on the central perceived color.


*Keywords:* Chromatic induction; Adaptation; Color coding cells; Computational model

## 1. Introduction

### 1.1. Overview

The appearance of a visual stimulus depends not only on the stimulus itself but also on other surrounding and remote stimuli. Induction (simultaneous contrast) and contrast induction are among the important appearance phenomena related to the spatial surrounding effects. Induction is a psychophysical phenomenon of the change in the appearance of a color (or an achromatic stimulus) caused by the presence of a surrounding average color (or luminance). The chromatic induction has also been defined as the color appearance caused by the surrounding visual stimuli or light adaptation mechanisms through gain control mechanisms (Shevell & Wei, 2000). Color contrast induction is the effect of modulating the perceived contrast of a central area due to the contrast of its surrounding area (D'Zmura & Singer, 1996; Singer & D'Zmura, 1994). Color contrast is the distance between colors in a perceptual uniform color space (Wyszecki & Stiles, 1982). Studies have also been conducted on the "intermixed" effect, i.e., the diverse effect of the perceived color resulting from a variegated (textured chromatic field) vs. a homogeneous surround where both surround areas are composed of the same average chromaticity and intensity (Brenner & Cornelissen, 2002; Shevell & Wei, 1998; Zaidi, Spehar, & DeBonet, 1998). In other words, the apparent color of a surface is affected not only by the average chromaticity of its surround but also by whether or not the surround is variegated or "articulated" in chromaticity domain (Brenner & Cornelissen, 2002; Shevell & Wei, 1998). The difference between the perceived stimulus and its immediate or remote surround is enhanced in the induction effect. Recent new

* Corresponding author. Tel.: +972 3 6409017; fax: +972 3 640 7939.
*E-mail address:* hedva@eng.tau.ac.il (H. Spitzer).

0042-6989/$ - see front matter © 2005 Elsevier Ltd. All rights reserved.
doi:10.1016/j.visres.2005.08.002

demonstrations possibly related to the White effect or to assimilation effects have been reported (Monnier & Shevell, 2003). Effects like the White effect, assimilation and their chromatic aspects are also influenced by background on the perceived color that yield opposite effects, which cause the color to be perceived similarly to the immediate surround. Our attempts to analyze these stimuli and effects are not included in the scope of this paper.

The chromatic induction and color constancy effects have been reported in recent psychophysical and physiological studies as being derived from the same neuronal mechanism and both are reflections of the chromatic adaptation mechanism (e.g., Fairchild, 1998; Shevell & Wei, 2000; Wachtler, Albright, & Sejnowski, 2001; Wachtler, Sejnowski, & Albright, 2003). Our current study proposes that different types of chromatic inductions (of color and chromatic contrast) are derived from mainly two types of adaptation mechanisms that occur at the retinal (color adaptation–first order) and cortical stage (chromatic contrast adaptation–second order). The purpose of adaptation is to maintain a high level of response sensitivity under different illuminations (or contrast) and stimulus conditions (contexts). Thus, an adaptation mechanism enables the system to maintain a high gain for a large stimulus range. Chromatic adaptation was defined by Fairchild (1998), as the "largely independent sensitivity regulation of the mechanisms of color vision," and in this context he related the color constancy effect as part of chromatic adaptation. In recent years, several studies reported that the chromatic and achromatic adaptation mechanisms can occur at different stages in the visual pathway and can have different temporal scales, including very fast mechanisms of around 50–500 ms (For example, Hayhoe & Wenderoth, 1991; Hughes & DeMarco, 2003; Rinner & Gegenfurtner, 2000; Shapiro, Beere, & Zaidi, 2003).

Even though the induction effects were thoroughly psychophysically investigated and have been related to adaptation mechanisms (or gain control mechanisms) (e.g., Shapiro et al., 2003; Shevell & Wei, 2000), there is no one accepted comprehensive computational model which demonstrates the different types of color and chromatic contrast induction effects (and color constancy effect). The lack of an accepted model might be, in part, the result of unknown or disputed physiological mechanisms that play a role in the induction effects (see below). In the following chapters we supply relevant physiological and psychophysical backgrounds that relate to each type of induction effect.

### 1.2. Color induction

Color perception is influenced not only by adjacent, but also by more remote non-contiguous regions (remote regions) within a visual scene. The influence of the color of peripheral areas on the perceived color of a central area is regarded here as the manifestation of the first order of color adaptation mechanism. There are electrophysiological findings which show this effect on the cells' responses, through stimuli located in peripheral area that extend far beyond the borders of the classical receptive field (Figs. 1A and B) of each of the color-coding cells, at different levels in the visual pathway (Creutzfeldt, Crook, Kastner, Li, & Pei, 1991a; Creutzfeldt, Kastner, Pei, & Valberg, 1991b; Kaplan & Benardete, 2001; Solomon, Peirce, & Lennie, 2004; Ts'o & Gilbert, 1988; Wachtler et al., 2003). Furthermore, Wachtler and his colleagues (2003) found recently that single neurons in primary visual cortex (area V1) of alert monkeys showed that chromatic tuning properties varied significantly in most neurons when the stimuli were presented on a colored background. It should also be noted that contrary to the above results, Solomon and his colleagues (2004) found that neither in cells of V1 nor in V2 did the surround regions alter the chromatic tuning of the classical receptive field. Wachtler and his colleagues (2003) suggested the possibility of the remote effect deriving from an earlier mechanism, i.e., retinal source. These suggestions concur with the findings of Creutzfeldt and his colleagues (Creutzfeldt et al., 1991a; Creutzfeldt et al., 1991b) and with the assumptions that our model relate to the contribution of the "remote" area, which extends beyond the classical receptive fields of the color opponent cells (Figs. 1A and C). This "remote" area relates to the first order of adaptation in our model.

Several psychophysical studies have characterized the induction effect as the effect of a shift in color appearance toward the complementary direction of the inducing stimulus (Krauskopf, Zaidi, & Mandler, 1986; Semo, Rosenbluth, & Spitzer, 1998; Webster & Mollon, 1995). This trend was found in the three cardinal as well as non-cardinal color directions, (Krauskopf et al., 1986), although exceptions have been shown in earlier studies using different paradigms (see review in Ware & Cowan, 1987).

The neuronal locus of color induction has been continually debated (Zaidi, 1999). In recent years, it has been accepted that a complementary color shift has a cortical (high level) origin, since the building blocks in the retina are the opponent color-coding cells (Fig. 1A). These can cause only an opponent shift in color (for example, a reddish surround region would cause a color shift towards a greenish color to the central achromatic region) and presumably cannot produce a complementary color shift (for example, reddish surround would cause a color shift towards cyanish to the central achromatic region), (Krauskopf et al., 1986; Zaidi, 1999). Since "Color induction" is widely accepted as being associated with the phenomenon of color constancy and with the manifestation of complementary colors to the surrounding stimuli colors, the mechanisms' site of both effects has been disputed in the literature.

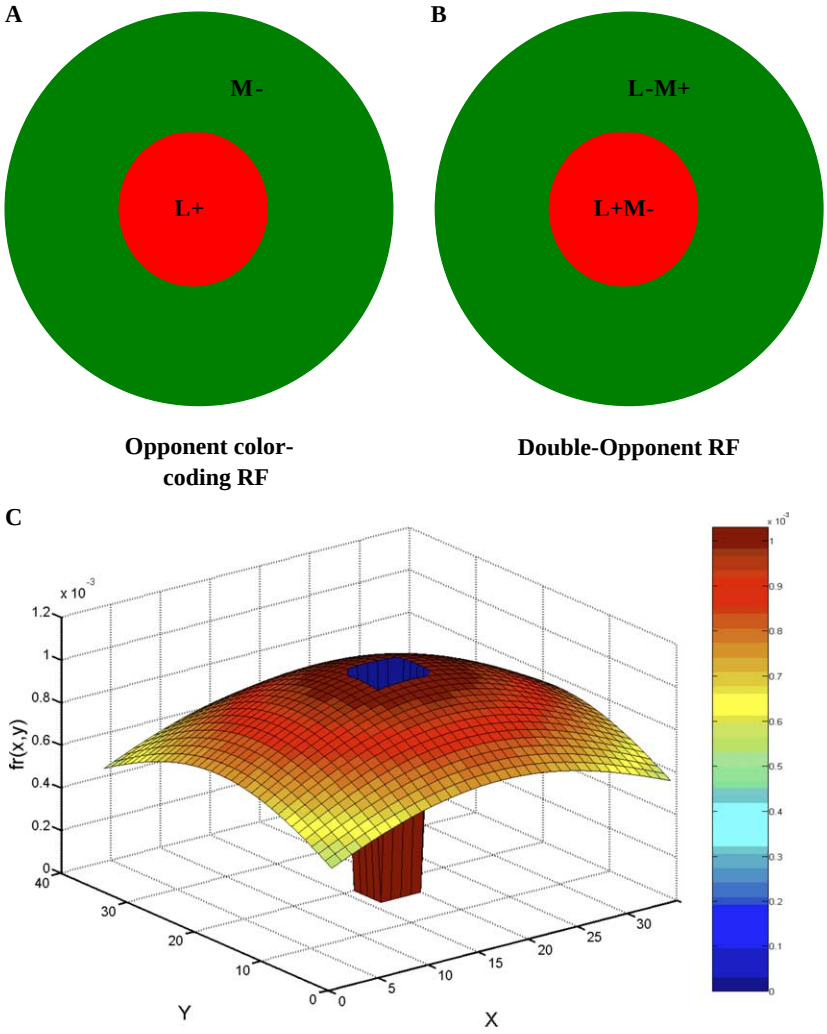


Fig. 1. Spatial structure of the receptive fields of one color-coding cell. (A) Retinal color-opponent receptive field. (B) Cortical "classical" double-opponent receptive field. The figure shows only units with L centers, as an example. (C) Demonstration of the normalized weight function of the remote area of the opponent receptive field. This area extends beyond the classical receptive field, i.e., beyond the center and surround receptive fields' areas (blue area in the center of the plot). The colors represent the value of the weight function at each specific location, according to the color-bar, Eqs. (13) and (14).

In this study we contest the logic of the visual locus of color induction and its accompanying effect of perceived complementary color, due to the adaptation mechanism (of the first order). This has been tested according to the model predictions. This part of the model is based on the building blocks as suggested in a previous model for color constancy (Spitzer & Rosenbluth, 2002; Spitzer & Semo, 2002). Our computational model has been tested to validate whether both the effects of color induction and color constancy are caused by the same adaptation mechanism.

### 1.3. Contrast–contrast induction

The influence of the color contrast of peripheral areas on the perceived contrast of a central area has been regarded as a color adaptation of the second order. Psychophysical and electrophysiological findings show the existence of the second-order adaptation, i.e., contrast–contrast adaptation, with basic adaptation properties that share somewhat similar properties to first-order effects, comparable to the role of the remote area (Chubb, Sperling, & Solomon, 1989; De Bonet & Zaidi, 1997; Schein & Desimone, 1990; Singer & D'Zmura, 1994; Zaidi, 1999). The color contrast induction findings imply the existence of an interocular transfer of color contrast induction, suggesting a cortical locus for contrast induction (Singer & D'Zmura, 1994). More direct evidence on the locus of the effect stemmed from findings on the remote areas, which are located in areas V1 (Wachtler et al., 2003) and V4 outside the "classical receptive field" of color-coding cells (Schein & Desimone, 1990). This effect is probably not only restricted to double opponent cells (Fig. 1B).

### 1.4. The model principles

To test our model's predictions for the above experimental effects, we developed the model as building blocks, based on adaptation mechanisms and color-coding receptive fields in the retina and the cortical level. The two suggested color adaptation mechanisms (the first and the second orders) are modeled as gain control mechanisms based on the "curve-shifting" effect, that is the transition from one response curve to another, resulting from a change in the light intensity (or color) of the local receptive field and its remote area, to obtain a higher gain in the new light intensity (Dahari & Spitzer, 1996; Sakmann & Creutzfeldt, 1969; Shapley & Enroth-Cugell, 1984; Spitzer & Rosenbluth, 2002; Spitzer & Semo, 2002). In the color contrast part of the model the "curve-shifting" mechanism relates to an increase in the color contrast rather than to the color or its intensity, as in the first part of the model and our previous models. The two adaptation mechanisms are automatic and are performed as a gain control mechanisms.

The receptive field, which encodes color contrast, should consist of both chromatic and spatial properties. The retinal building blocks, i.e., the color opponent cells, are largely able to differentiate between colors, but not necessarily differentiate between their spatial properties. This can be represented by comparing the color-coding cell response to a diffuse and a local color stimulus in the center of the receptive field. These two different spatial stimuli yield a similar cell response, and thus this cell type is not able to quantify color contrast. However, a distinction between different chromatic contrasts can be obtained by cortical "classical" (or oriented) double opponent receptive fields (Fig. 1B) that yield a different response to the above example of diffuse and local color stimuli. Therefore, these double opponent receptive fields were applied for the second part of the model and the second order of adaptation, which are associated with the chromatic contrast modulation due to the surround areas.

The entire model presents the two stages of adaptation mechanisms that demonstrate the prediction of the above two types of induction effects and the variegated induction effect (effect of texture on perceived color, see above). The model is based on the retinal (for the first order of adaptation) and cortical (for the second order of adaptation) color-coding receptive fields.

For improved clarification, a current brief description of the actual principles of the model is presented. The first part of the model (Fig. 2) includes the first order of the adaptation mechanism, that is based on the retinal color-coding cells, the opponent cells ($L^+/M^-$, $M^+/L^-$ and $S^+/(M^+ + L^-)$), Fig. 1A. The two sub-regions of the receptive field, center and surround regions are adapted autonomously by separate mechanisms. The adaptation of the first order includes two adaptation components, local (relating to the receptive field) and remote (relating to the remote area which extends beyond the size of the classical receptive field).

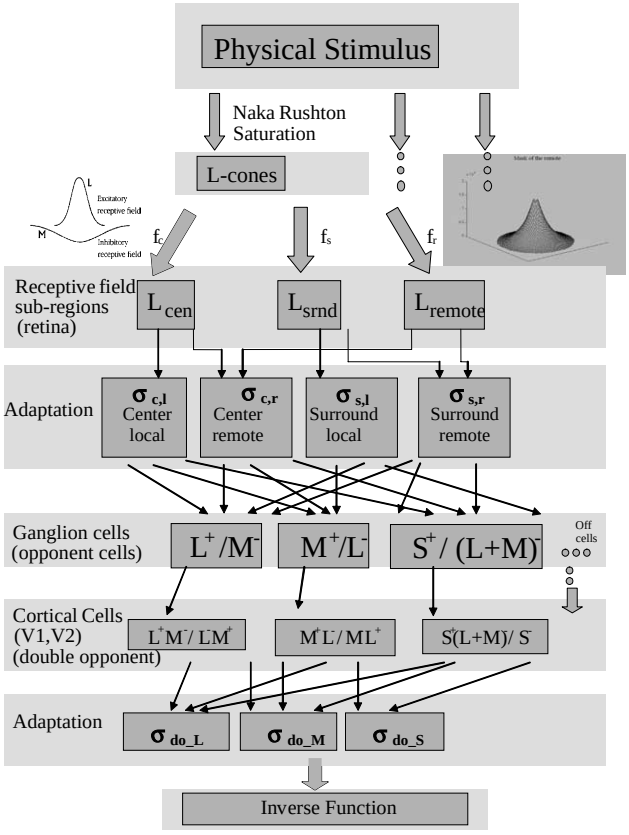


Fig. 2. Schematic diagram of the suggested model.

The second part of the model (Fig. 2) refers to the processing of color contrast and the building blocks of the cortical color-coding cells, the classical double opponent cells ($L^+/M^-/L^-/M+$, $M^+/L^-/M^-/L^+$ and $S^+/(M^+ + L^-)^-/S^-/(M^+ + L^-)^+$), Fig. 1B. To simplify the model, we related only to these types of receptive field in the model, even though additional types have been found in recent years, but largely disputed regarding their distribution in different visual cortical areas. The model assumes that the double-opponent receptive field type is fed by an On-center cell type receptive field to its center region, and that an Off-center cell type that has the same chromaticity properties as its surround region.

### 1.5. The model goals

One of the main goals of this study was to test predictions of different chromatic induction effects from the adaptation model of the first and second orders. (Lightness induction effects have not been analyzed within the scope of this paper.) In the first part of this study, we tested the color induction effects and examined whether they would predict the experimentally observed complementary nature of the induction effect. The prediction

based mainly on the first part of the model, consequently assumed that both the color induction and color constancy are derived from the same mechanism. This was also tested by examining the same mechanism's ability to predict both effects.

The model was also tested for the second order of induction effects, the chromatic contrast–contrast induction effect (D'Zmura & Singer, 1996; Singer & D'Zmura, 1994), based mainly on the second part of the model, i.e., the second order of adaptation. It was also tested for the prediction of the induction of textured chromatic surround on the perceived color (Brenner & Cornelissen, 2002; Brown & MacLeod, 1997; Shevell & Wei, 1998). For this prediction the application of both orders of adaptation mechanisms is crucial. The first order serves to enhance the differences between the stimulus (it color or intensity) and its surrounding area and the second order enhances the contrast and therefore the differences in texture between the stimulus and its surrounding area. As far as we know, there is no previously proposed comprehensive model in the literature that describes all the above chromatic induction effects. Former models did not confront predictions of a set of induction effects in a single model nor (as far as we know) did they challenge these effects on physiological receptive fields and adaptation mechanisms. Furthermore, no previous biological model has succeeded to predict induction, color constancy and color contrast enhancement of real images.

## 2. The model

The model is presented in three main stages, see Fig. 2. The first stage (Section 2.1) describes the transformation of visual stimuli into responses of three types of retinal ganglion On or Off center cells, which will be referred to as color-coding cells or opponent cells. The second stage (Section 2.2) describes the cortical double-opponent color-coding cells, which are fed by the responses of the first stage, and the remote adaptation mechanism that acts on their responses. The third stage (Section 2.3), which is performed through an inverse function, calculates a transformation of these cells' activity levels to a perceived image, in a standard CIE notation (XYZ) or RGB space.

### 2.1. Responses of three types of On-center color-coding cells, the first adaptation order

The retinal ganglion cells' responses form the last chain of data processing in the retina. They receive their input from the cones through several processing layers. These cells have a color-opponent receptive field (RF) with a center-surround spatial structure. The model uses the three most common color-coding types in the retina. These cell types are labeled $L^{+}M^{-}$, $M^{+}L^{-}$ and $S^{+}(L+M)^{-}$, with L, M, and S indicating long, medium and short wavelength sensitivity, respectively. For example, an $S^{+}(L+M)^{-}$ cell has an excitatory S ("blue") response in its center and an inhibitory (L+M) ("yellow") response in its surround.

The input to the cone level comprises the spectral composition of the light reaching the retina, when an illumination falls on and is reflected from surfaces of objects. The field of view is mapped by the three types of cones, L, M, and S. The quantum catch of each of the three cone types, $L_{\text{cone}}$, $M_{\text{cone}}$ and $S_{\text{cone}}$, is expressed by an inner product of the cone pigment sensitivities, the spectral composition of the illumination and the reflectance properties of the surface (Wyszecki & Stiles, 1982).

The spatial response profile of the two sub-regions of the retinal ganglion RF, "center" and "surround", is expressed by the commonly used difference-of-Gaussians (DOG), performed only after each sub-region is adapted, as follows: The "center" signals for the three spectral regions, $L_{\text{cen}}$, $M_{\text{cen}}$ and $S_{\text{cen}}$, that feed the retinal ganglion cells' level are defined as an integral of the cones' quantum catches, $L_{\text{cone}}$, $M_{\text{cone}}$ and $S_{\text{cone}}$ over the center sub-region, with a Gaussian decaying spatial weight function, $f_{\text{c}}(x-x_0,\ y-y_0)$ (Shapley & Enroth-Cugell, 1984):

$$
\begin{aligned}
L_{\text{cen}}(x_0,y_0) &= \iint_{\text{cen-area}} L_{\text{cone}}(x,y) f_{\text{c}}(x-x_0,y-y_0)\,\mathrm{d}x\,\mathrm{d}y,\\
M_{\text{cen}}(x_0,y_0) &= \iint_{\text{cen-area}} M_{\text{cone}}(x,y) f_{\text{c}}(x-x_0,y-y_0)\,\mathrm{d}x\,\mathrm{d}y,\\
S_{\text{cen}}(x_0,y_0) &= \iint_{\text{cen-area}} S_{\text{cone}}(x,y) f_{\text{c}}(x-x_0,y-y_0)\,\mathrm{d}x\,\mathrm{d}y,
\end{aligned}
\tag{1}
$$

while the variables $L_{\text{cen}}$, $M_{\text{cen}}$, $S_{\text{cen}}$ at locations $x_0$, $y_0$ represent the response of the center area of the receptive field of each cell type which is centered at location $x_0$, $y_0$. The following equations are similarly expressed,but in order to simplify $x_0$, $y_0$ will be substituted as: $x_0 = y_0 = 0$. $f_{\text{c}}$ is defined by:

$$
f_{\text{c}}(x,y) = \frac{\exp[-(x^2+y^2)/\rho_{\text{cen}}^2]}{\pi\rho_{\text{cen}}^2}, \quad x,y \in \text{center area},
\tag{2}
$$

where $\rho$ represents the radius of the center region of the receptive field of the color-coding cells. The "center" can be stimulated by as little as a single cone, as frequently occurs in the fovea (the center of the gaze).

The "surround" signals of On-center color-coding cells, $L_{\text{srnd}}$, $M_{\text{srnd}}$ and $(L+M)_{\text{srnd}}$ represent the surround sub-region of these receptive fields. The three "surround" signals are similarly defined, with the outer diameter of the annular "surround" being usually three

times larger than that of the "center" (Shapley & Enroth-Cugell, 1984):

$$\begin{aligned} L_{\text{srnd}} &= \iint_{\text{surround area}} L_{\text{cone}} f_{\text{s}}(x,y)\,\mathrm{d}x\,\mathrm{d}y, \\ M_{\text{srnd}} &= \iint_{\text{surround area}} M_{\text{cone}} f_{\text{s}}(x,y)\,\mathrm{d}x\,\mathrm{d}y, \\ (L+M)_{\text{srnd}} &= \iint_{\text{surround area}} \frac{L_{\text{cone}}+M_{\text{cone}}}{2} f_{\text{s}}(x,y)\,\mathrm{d}x\,\mathrm{d}y, \end{aligned} \tag{3}$$

where $f_{\text{s}}$ is defined as a decaying exponent over the surround region (similar to the following definition of $f_{\text{r}}$ (Eq. (5)) but on the relevant region). The total weight of $f_{\text{c}}$ and $f_{\text{s}}$ is 1.

The "remote" signal ($L_{\text{remote}}$, $M_{\text{remote}}$, $S_{\text{remote}}$ and $(L+M)_{\text{remote}}$) represents the peripheral area that extends far beyond the RF borders of the color-coding cells and is defined as an integral of the cones' quantum catches over the remote area, with a different Gaussian decaying spatial weight function (Creutzfeldt et al., 1991a; Dahari & Spitzer, 1996; Spitzer & Rosenbluth, 2002; Spitzer & Semo, 2002). The "remote" area, Fig. 1C, has the shape of annulus, concentric to that of the "center" and of the "surround". The inner diameter of the "remote" is equal to the external diameter of the "surround" and therefore does not overlap the "center" or the "surround". This remote signal is a cardinal part of the adaptation mechanism (that will be described below), $L_{(\text{remote})}$, $M_{(\text{remote})}$ $S_{(\text{remote})}$ and $(L+M)_{(\text{remote})}$. The four "remote" signals that feed the retinal ganglion cells level:

$$\begin{aligned} L_{(\text{remote})} &= \iint_{\text{remote area}} L_{\text{cone}}(x,y) f_{\text{r}}(x,y)\,\mathrm{d}x\mathrm{d}y, \\ M_{(\text{remote})} &= \iint_{\text{remote area}} M_{\text{cone}}(x,y) f_{\text{r}}(x,y)\,\mathrm{d}x\,\mathrm{d}y, \\ S_{(\text{remote})} &= \iint_{\text{remote area}} S_{\text{cone}}(x,y) f_{\text{r}}(x,y)\,\mathrm{d}x\,\mathrm{d}y, \\ (L+M)_{(\text{remote})} &= \iint_{\text{remote area}} \frac{L_{\text{cone}}+M_{\text{cone}}}{2} f_{\text{r}}(x,y)\,\mathrm{d}x\,\mathrm{d}y, \end{aligned} \tag{4}$$

where $f_{\text{r}}$, the remote weight function, is defined by

$$f_{\text{r}}(x,y) = \frac{\exp\left[-\sqrt{(x^2+y^2)}/K_{\text{remote}}\right]}{A_{\text{remote}}}, \quad x,y \in \text{remote area}, \tag{5}$$

where $k_{\text{remote}}$ is constant and $A_{\text{remote}}$ is a factor of normalization to a total weight of 1.

A color-coding cell response (Eq. (6)) is the subtraction between the responses of the center and the surround of each retinal ganglion cell type after the adaptation (according to the Naka–Rushton equation) for each sub-region separately (Dahari & Spitzer, 1996; Shapley & Enroth-Cugell, 1984) as shown in Fig. 2. The adaptation process for each sub-region is performed according to the content of the sub-region and its remote area, as explained below and also reflects the history of the stimulation of the relevant region and its remote area, according to the curve-shifting mechanism, Fig. 3 (Dahari & Spitzer, 1996; Sakmann & Creutzfeldt, 1969; Spitzer & Semo, 2002). For On-center cells the response is expressed as $R_{\text{op}(L^+M^-)}$, $R_{\text{op}(M^+L^-)}$ and $R_{\text{op}(S^+(L+M)^-)}$, and correspondingly for Off-center cells" type. The response of each of the On-center color-coding cells was therefore expressed by:

$$\begin{aligned} R_{\text{op}(L^+M^-)}(t) &= \frac{L_{\text{cen}}}{L_{\text{cen}}+\sigma_{L^+M^--\text{cen}}(t)} - \frac{M_{\text{srnd}}}{M_{\text{srnd}}+\sigma_{L^+M^--\text{srnd}}(t)}, \\ R_{\text{op}(M^+L^-)}(t) &= \frac{M_{\text{cen}}(t)}{M_{\text{cen}}+\sigma_{M^+L^--\text{cen}}(t)} - \frac{L_{\text{srnd}}}{L_{\text{srnd}}+\sigma_{M^+L^--\text{srnd}}(t)}, \\ R_{\text{op}(S^+(L+M)^-)}(t) &= \frac{S_{\text{cen}}}{S_{\text{cen}}+\sigma_{S^+(L+M)^--\text{cen}}(t)} - \frac{(L+M)_{\text{srnd}}}{(L+M)_{\text{srnd}}+\sigma_{S^+(L+M)^--\text{srnd}}(t)}, \end{aligned} \tag{6}$$

where $L$, $M$, $S$ is the signal (of each of the color-coding cells) feeding the "center" (Eq. (1)) or the "surround" sub-regions, $\sigma$ is used here as the adaptation factor instead of the "saturation constant" of the Naka–Rushton equation (Dahari & Spitzer, 1996; Spitzer & Semo, 2002).

The adaptation function $\sigma$ depends on the current stimulation of each sub region and its remote area and on the temporal history of these stimulations, and is determined through a dynamic time-filter (Dahari & Spitzer, 1996). A change in $\sigma$ produces a gain control effect, which is equivalent to the curve shift of the "response vs. log contrast or illumination" curve, Fig. 3B, which has been shown experimentally (Sakmann & Creutzfeldt, 1969; Shapley & Enroth-Cugell, 1984). A curve-shifting effect is the transition from one response curve to another, due to a change in contrast (or color or light intensity), in order to obtain a higher gain of the new stimulus range, Fig. 3. The adaptation is reflected in a shift of the response curve as a function of time (Fig. 3A). Consequently, each time a new range of input intensities to a color channel is viewed, given the long-lasting stimulation of the change from the previous stimulation, a curve shift will occur, bringing the system to a new adaptation state. This curve shift takes place according to the time-filter, causing an apparent

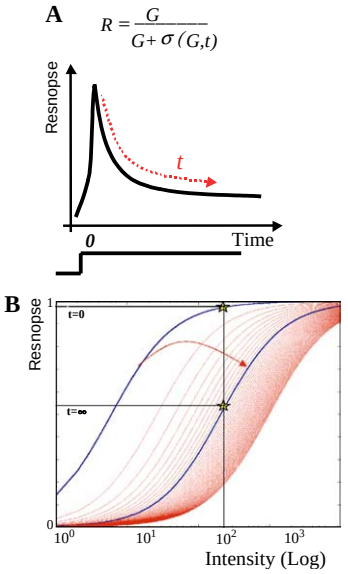


Fig. 3. Illustration of the biological gain control, i.e., the curve-shifting mechanism of "response vs. log intensity" curve, which was applied as an adaptation mechanism. The curves illustrate the response of each sub-region of a receptive field as a function of time and the intensity of the relevant chromatic stimulus in this area at various adaptational levels. (A) The curve shift causes an apparent decaying function of the response (Eq. (6) in reference to the time dependence of $\sigma$, (Spitzer & Semo, 2002)), to a steady and spatially diffused stimulus (see in the bottom of the curve). This stimulus causes an abrupt increase in cell response and then decay due to the adaptation (red dashed curve). (B) The curve-shifting mechanism is the transition from one response curve to another, resulting from a change in the light intensity (or color) of the local receptive field and its remote area, in order to obtain a higher gain in the new light or contrast intensity. The dark (blue) left curve represents the normalized curve response before the adaptation. The right dark curve represents the response curve after the adaptation (see text). The yellowish stars illustrate a transition of the response to a specific intensity value before the adaptation, $t = 0$ (upper star), and after the completion of the adaptation, at $t = \infty$, see text. The red dashed line illustrates the temporal behavior of the curve-shifting.

decaying function of the response. The dynamic adaptation is caused by both mechanisms of the local and remote adaptation. In the current study, we only applied stimulations for the steady state responses, while the whole model includes the temporal properties as well, which play a role in the visual system for other visual effects (Spitzer & Semo, 2002).

The dependence of $\sigma$ as a function of the history of the stimulation in this study was composed of local, $\sigma_{\text{local}}$ and remote $\sigma_{\text{remote}}$ components. The model was designed to comply with Weber's law (which states that there is a constant proportion by which a standard stimulus must be increased in order to detect a response change to local adaptation) and thus $\sigma_{\text{local}}$ and $\sigma_{\text{remote}}$ were defined accordingly (Dahari & Spitzer, 1996; Spitzer & Semo, 2002) as specifically described below (for example, for the color-coding $L^+M^-$ cell type):

$$\begin{aligned}
&\sigma_{L^+M^-\text{–cen}} = \sigma_{L^+M^-\text{–cen–local}} + \sigma_{L^+M^-\text{–cen–remote}},\\
&\sigma_{L^+M^-\text{–srdn}} = \sigma_{L^+M^-\text{–srdn–local}} + \sigma_{L^+M^-\text{–srdn–remote}},\\
&\text{where}\\
&\sigma_{L^+M^-\text{–cen–local}} = \alpha_{\text{cen}} L_{b_{\text{cen}}} + \beta_{\text{cen}},\\
&\sigma_{L^+M^-\text{–cen–remote}} = c_{\text{cen}} L_{b_{\text{remote}}},\\
&\text{and}\\
&\sigma_{L^+M^-\text{–srdn–local}} = \alpha_{\text{srdn}} M_{b_{\text{srdn}}} + \beta_{\text{srdn}},\\
&\sigma_{L^+M^-\text{–srdn–remote}} = c_{\text{srdn}} M_{b_{\text{remote}}},
\end{aligned} \tag{7}$$

where $\alpha$, $\beta$ and $c$ are constants, with different values for the "center" and the "surround". $L_{\text{b}}$, $M_{\text{b}}$ and $S_{\text{b}}$ are the adapting response components of the corresponding sub-regions. (Note that expressions indexed with "b" refer to a component that is a function of the history of the stimulation.) With regard to still images in the current study, only responses of the stimuli, which are constant in time and have already reached a steady state, were analyzed. When substitution of $t = \infty$ in Eq. (7) is applied, the adaptation factors are then expressed by (as an example, for $L^+M^-$ color opponent cell):

$$\begin{aligned}
&\sigma_{L^+M^-\text{–cen}}(t=\infty) = a_{\text{cen}} L_{\text{cen}} + b_{\text{cen}} + c_{\text{cen}} L_{\text{remote}},\\
&\sigma_{L^+M^-\text{–srdn}}(t=\infty) = a_{\text{srdn}} M_{\text{srdn}} + b_{\text{srdn}} + c_{\text{srdn}} M_{\text{remote}},
\end{aligned} \tag{8}$$

when $a = \alpha + 1$ and $b = \beta$ of the center and surround regions. The steady-state responses of the color-coding cells are expressed by substituting Eq. (8) into Eq. (6). (The parameter "$a$" for each receptive field region was redefined as "$a$"$-1$ for the sake of algebraic simplicity.)

$$\begin{aligned}
R_{\text{op}(L^+M^-)} &= \frac{L_{\text{cen}}}{a_{\text{cen}} L_{\text{cen}} + b_{\text{cen}} + c_{\text{cen}} L_{\text{remote}}} - \frac{M_{\text{srnd}}}{a_{\text{srdn}} M_{\text{srdn}} + b_{\text{srdn}} + c_{\text{srdn}} M_{\text{remote}}},\\
R_{\text{op}(M^+L^-)} &= \frac{M_{\text{cen}}}{a_{\text{cen}} M_{\text{cen}} + b_{\text{cen}} + c_{\text{cen}} M_{\text{remote}}} - \frac{L_{\text{srnd}}}{a_{\text{srdn}} L_{\text{srdn}} + b_{\text{srdn}} + c_{\text{srdn}} L_{\text{remote}}},\\
R_{\text{op}(S^+(L^+M)^-)} &= \frac{S_{\text{cen}}}{a_{\text{cen}} S_{\text{cen}} + b_{\text{cen}} + c_{\text{cen}} S_{\text{remote}}} - \frac{(L+M)_{\text{srnd}}}{a_{\text{srdn}} (L+M)_{\text{srnd}} + b_{\text{srdn}} + c_{\text{srdn}} (L+M)_{\text{remote}}}.
\end{aligned} \tag{9}$$

### 2.2. Double-opponent cells, the second order

The color-opponent cells' responses (Eq. (9)) (from the previous stage) feed the cortical double-opponent cells. Three types of double opponent cells were considered in the model (Introduction). The double-opponent receptive field is composed of a center and surround region. Its center signal (termed here as $L_{(\text{do-c})}$ ("do-center" (do-c) signal)) is composed of the first group of On-center color opponent cells (for example, $L^+M^-$,

the group that subtracts the $M$ surround responses from $L$ center responses) and is located in a do-center area. Its surround signal (termed here as $L_{(\text{do-s})}$ (''do-surround'' (do-s) signal)) is composed of the corresponding group of Off-center cells (e.g., $L^-M^+$) and is located in a do-surround area (Fig. 1). The mathematical expressions for the three ''do-center'' (Eq. (10)) and ''do-surround'' (Eq. (11)) responses are given by:

$$\begin{aligned}
L_{(\text{do-c})} &= \iint_{\text{center-do-area}} R_{\text{op}(L^+M^-)}(x,y) f_{(\text{do-c})}(x,y)\,\mathrm{d}x\,\mathrm{d}y,\\
M_{(\text{do-c})} &= \iint_{\text{center-do-area}} R_{\text{op}(M^+L^-)}(x,y) f_{(\text{do-c})}(x,y)\,\mathrm{d}x\,\mathrm{d}y,\\
S_{(\text{do-c})} &= \iint_{\text{center-do-area}} R_{\text{op}(S^+(L+M)^-)}(x,y) f_{(\text{do-c})}(x,y)\,\mathrm{d}x\,\mathrm{d}y,
\end{aligned} \tag{10}$$

$$\begin{aligned}
L_{(\text{do-s})} &= \iint_{\text{surround-do-area}} R_{\text{op}(L^-M^+)}(x,y) f_{(\text{do-s})}(x,y)\,\mathrm{d}x\,\mathrm{d}y,\\
M_{(\text{do-s})} &= \iint_{\text{surround-do-area}} R_{\text{op}(M^-L^+)}(x,y) f_{(\text{do-s})}(x,y)\,\mathrm{d}x\,\mathrm{d}y,\\
S_{(\text{do-s})} &= \iint_{\text{surround-do-area}} R_{\text{op}(S^-(L+M)^+)}(x,y) f_{(\text{do-s})}(x,y)\,\mathrm{d}x\,\mathrm{d}y.
\end{aligned} \tag{11}$$

Note that the ''$R(x,y)$'' responses above are actually the opponent cell responses (Eq. (9)) of a cell with its receptive field centered at $x,y$ location. The center sub-region $f_{(\text{do-c})}$ has a Gaussian spatial-weight function. For the surround sub-region the weight function has been similarly assessed as in the first order of adaptation.

Before adaptation the double-opponent responses (or ''do-outputs'') of the three On-center, double-opponent color-coding cells were given by:

$$\begin{aligned}
L_{(\text{do})} &= L_{(\text{do-c})} - M_{(\text{do-s})},\\
M_{(\text{do})} &= M_{(\text{do-c})} - L_{(\text{do-s})},\\
S_{(\text{do})} &= S_{(\text{do-c})} - \frac{(L_{(\text{do-s})} + M_{(\text{do-s})})}{2},\\
Y_{(\text{do})} &= \frac{(L_{(\text{do-c})} + M_{(\text{do-c})})}{2} - S_{(\text{do-s})},
\end{aligned} \tag{12}$$

where $L_{(\text{do})}$, $M_{(\text{do})}$, $S_{(\text{do})}$ represent the responses of the three types of double opponent cells (before the adaptation), for example, $L_{(\text{do})}$ represents the response of $L^+/M/L^-/M+$ cell. For the simulation we chose to use the fourth ($Y_{(\text{do})}$, yellow) do-output obtained by subtracting the blue do-surround from the yellow do-center.

### 2.2.1. Remote area

The ''remote'' signal represents the peripheral area that extends far beyond the borders of the double-opponent classical receptive field of the V1 (Wachtler et al., 2003) or V4 area (Schein & Desimone, 1990), see Introduction. The ''remote'' area, located outside the ''classical'' RF region, is composed of an annulus-like shape around the entire RF region. The four remote signals ($L_{(\text{do-remote})}$, $M_{(\text{do-remote})}$, $S_{(\text{do-remote})}$ and $(L+M)_{(\text{do-remote})}$) were defined as the inner product of each absolute response at each location of the remote area of the double-opponent cell signal or as a convolution for an image. The adaptation of the second order is performed after subtracting the center and surround sub-regions from the double opponent cell. Utilizing such remote adaptation and absolute signals enables the system to relate the double opponent responses as a contrast quantifier. Application of absolute response was also used in the literature for expressing achromatic contrast through a rectification stage, for example, for cortical sub-regions of complex cell responses (e.g., Spitzer & Hochstein, 1985). The four ''remote'' signals, $L_{\text{remote}}$, $M_{\text{remote}}$, $S_{\text{remote}}$ and $(L+M)_{\text{remote}}$ that fed the double-opponent cells level, are defined as:

$$\begin{aligned}
L_{(\text{do-remote})} &= \iint_{\text{remote area}} |L_{(\text{do})}(x,y)| f_{\text{r}}(x,y)\,\mathrm{d}x\,\mathrm{d}y,\\
M_{(\text{do-remote})} &= \iint_{\text{remote area}} |M_{(\text{do})}(x,y)| f_{\text{r}}(x,y)\,\mathrm{d}x\,\mathrm{d}y,\\
S_{(\text{do-remote})} &= \iint_{\text{remote area}} |S_{(\text{do})}(x,y)| f_{\text{r}}(x,y)\,\mathrm{d}x\,\mathrm{d}y,\\
(L+M)_{(\text{do-remote})} &= \iint_{\text{remote area}} |Y_{(\text{do})}(x,y)| f_{\text{r}}(x,y)\,\mathrm{d}x\,\mathrm{d}y,
\end{aligned} \tag{13}$$

where $L_{(\text{do})}(x,y)$, $M_{(\text{do})}(x,y)$, $S_{(\text{do})}(x,y)$ and $Y_{(\text{do})}(x,y)$ are the responses at each $x,y$ location which act on the do-remote areas. $f_{\text{r}}$ was chosen as an exponentially decaying spatial-weight function. $f_{\text{r}}$ could also be chosen as a Gaussian function.

$$f_{\text{r}}(x,y) = \frac{\exp\left[-\sqrt{(x^2+y^2)}/K_{\text{remote}}\right]}{A_{\text{remote}}}. \tag{14}$$

$K_{\text{remote}}$ is a constant, which defines the slope of the weight function. $A_{\text{remote}}$ is a factor of normalization to a unit

$$A_{\text{remote}} = \iint_{\text{remote area}} \exp -\left(\frac{\sqrt{x^2+y^2}}{K_{\text{remote}}}\right). \tag{15}$$

### 2.2.2. Adaptation of second order

The color-coding double-opponent cells were adapted (Eqs. (16) and (17)) by a suggested remote adaptation mechanism in a manner similar to a mechanism based on psychophysical findings, as reported in Singer and D'Zmura (D'Zmura & Singer, 1996; Singer & D'Zmura, 1994) (Section 1). This contrast adaptation, although on

a different domain (contrast instead of intensity or color) is comparable to the adaptation at the retinal level.

The response of each of the adapted On-center color-coding double-opponent cells ($L_{(\text{do-a})}$, $M_{(\text{do-a})}$, $S_{(\text{do-a})}$ and $Y_{(\text{do-a})}$) is therefore expressed by Eq. (16) (illustrated for $L_{(\text{do-a})}$):

$$L_{(\text{do-a})} = R_{\max}\frac{L_{(\text{do})}}{|L_{(\text{do})}| + \sigma_{(\text{L-do-rmt})}(t)}, \tag{16}$$

where

$$\sigma_{(\text{L-do-rmt})}(t) = cL_{(\text{do-remote-b})}(t) + \beta, \tag{17}$$

and where $L_{\text{do-remote-b}}$ indicates the temporal dependence of $L_{\text{do-remote}}$ and determines the dynamic adaptation.

According to psychophysical findings, the adaptation of a specific color contrast channel is influenced not only by the remote area of the same spectral properties, but also to a lesser extent by the other contrast channels (Brenner & Cornelissen, 2002; Brown & MacLeod, 1997; Shevell & Wei, 1998; see also Introduction). Thus, an additional component was included in the adaptation factor of the second order. Accordingly, Eq. (17) is replaced by Eq. (18) and demonstrates the color contrast channel $L/M$:

$$\sigma_{(\text{L-do-rmt})}(t) = c_{\text{do}} \cdot L_{(\text{do-remote-b})}(t) + b_{\text{do}} + d_{\text{do}} \cdot S_{(\text{do-remote-b})}(t), \tag{18}$$

where $d_{do}$ represents the interaction channel adaptation, which is defined as less than 1. The same considerations and calculations were applied for the other color contrast channel, i.e., $S_{(\text{do})}$.

In this study we only simulated a steady-state response, when $t = \infty$ is applied, $L_{(\text{do-remote-b})}$, $M_{(\text{do-remote-b})}$ and $S_{(\text{do-remote-b})}$ are expressed as (illustrated for $L$ component):

$$L_{\text{do-remote-b}}(t = \infty) = L_{(\text{do-remote})} \tag{19}$$

Thus, the response of the double opponent cell after adaptation at steady state is achieved by substituting Eqs. (18) and (19) in Eq. (16):

$$L_{(\text{do-a})} = R_{\max} \times \frac{L_{(\text{do})}}{|L_{(\text{do})}| + c_{\text{do}} \cdot L_{(\text{do-remote})} + d_{\text{do}} \cdot S_{(\text{do-remote})} + b_{\text{do}}}. \tag{20}$$

$R_{\max}$ is the maximum response used as a normalization factor. The constant $c_{\text{do}}$ describes the degree of the "curve-shifting", i.e., it determines the shift of the response curve due to the remote signal. The rationale for the suggested adaptation is that the cell response will retain a high gain in the region of the current remote contrast (similar to the goal of the first-order adaptation but on a different domain). This logic holds for each receptive field region and thus enables the model or the algorithm to be locally adaptive.

### 2.3. Transformation of the adapted color cells' response to a perceived image

This procedure was used for inversely calculating the functions of the adapted double-opponent responses, then the opponent to cone responses and then the values of RGB scale, in order to observe the outcome of the perceived image. The following procedure of inverse function enables us to present the predicted perceived images of the different stimuli, which cause the induction effect. Thus, this procedure also enables quantitative estimation of the model's performance. The paragraph below describes the main principles and assumptions that prompted our performing the inverse function. The first and main assumption is related to the perceived color contrast component, termed by the triplet of $L'_{\text{do}}$ $M'_{\text{do}}$ $S'_{\text{do}}$. The assumption is that the contrast in the region of the double-opponent receptive field is equal to the contrast in its remote area. This is expressed as:

$$L'_{(\text{do-remote})} = |L'_{\text{do}}|M'_{(\text{do-remote})} = |M'_{\text{do}}|S'_{(\text{do-remote})} = |S'_{\text{do}}|. \tag{21}$$

The terms $L'$ $M'$ $S'$ with apostrophe relate to the inversed responses i.e., the suggested "perceived responses". This assumption was chosen in order to avoid contrast modulation when there is a uniform contrast in a stimulus, since in such specific stimulus conditions there is no psychophysical contrast modulation. Note that the "remote" signal of the double opponent receptive field, Eq. (4), express the chromatic contrast of this remote region. Thus, in order to obtain identical chromatic contrast value from perceived double opponent receptive fields' responses ($L'$, $M'$, $S'$) and their corresponding remote areas (regardless to their sign of response), absolute values were also taken from the perceived double opponent receptive fields' responses, Eq. (22). Accordingly, the new double opponent cells ($L'_{\text{do}}$ $M'_{\text{do}}$ $S'_{\text{do}}$) values in the inverse function were calculated with the above assumption on the remote effect. Thus:

$$\begin{aligned} R'_{(\text{do-a})} &= R_{\max}\frac{L_{(\text{do})}}{|L_{(\text{do})}| + c_{\text{do}}L_{(\text{do-remote})} + d_{\text{do}} \cdot S_{(\text{do-remote})} + b_{\text{do}}} \\ &= R_{\max}\frac{L'_{\text{do}}}{|L'_{\text{do}}| + c_{\text{do}}|L'_{\text{do}}| + b_{\text{do}}}. \end{aligned} \tag{22}$$

The extraction of $L'_{\text{do}}$ is

$$L'_{\text{do}} = \frac{b_{\text{do}} \cdot L_{\text{do}}}{c_{\text{do}} \cdot (L_{\text{do-remote}} - |L_{\text{do}}|) + d_{\text{do}} \cdot S_{(\text{do-remote})} + b_{\text{do}}}. \tag{23}$$

Although the RF of the double-opponent cell is composed of both a "center" and a "surround" sub-region, the change in the calculated perceived contrast was ascribed only to the spatial coordinates of the "center" sub-region. Therefore,

$$R'_{\mathrm{op}(L^+M^-)} = L'_{\mathrm{do\text{-}c}} = L'_{\mathrm{do}} + M_{\mathrm{do\text{-}s}}. \tag{24}$$

The inverse function of the opponent cells' responses to cone values was performed assuming that a uniform achromatic surface was presented in their "remote" area (Spitzer & Rosenbluth, 2002; Spitzer & Semo, 2002). This is expressed as:

$$\begin{aligned} R'_{\mathrm{op}(L^+M^-)-\mathrm{cen}} &= \frac{L'_{\mathrm{cen}}}{a_{\mathrm{cen}}L'_{\mathrm{cen}} + b_{\mathrm{cen}} + c_{\mathrm{cen}}L'_{\mathrm{remote}}} \\ &= R'_{\mathrm{op}(L^+M^-)} \\ &\quad + \frac{U_{\mathrm{srnd}}}{a_{\mathrm{srdn}}U_{\mathrm{srdn}} + b_{\mathrm{srdn}} + c_{\mathrm{srdn}}U_{\mathrm{remote}}}. \end{aligned} \tag{25}$$

And extracting $L'_{\mathrm{cen}}$:

$$L'_{\mathrm{cen}} = \frac{R'_{\mathrm{op}(L^+M^-)-\mathrm{cen}} \cdot (c_{\mathrm{cen}}U_{\mathrm{remote}} + b_{\mathrm{cen}})}{1 - a_{\mathrm{cen}} \cdot R'_{\mathrm{op}(L^+M^-)-\mathrm{cen}}}, \tag{26}$$

while $U$ represents the calculated luminance of the corresponding surround and remote area of the opponent receptive field. These values were calculated according to the original luminance in these areas on the assumption that the visual system interprets the color of an object as it would the appearance of a perceived color in void. The adapted cone responses may then be converted to the CIE RGB color space or to any other color space (Wyszecki & Stiles, 1982).

## 3. Results

### 3.1. Parameters

Physiological findings show that the specific parameters can be varied from cell to cell, even among cells in the same visual stage and cells of the same cell type, according to physiological findings (e.g., Dahari & Spitzer, 1996; Schein & Desimone, 1990; Shapley & Enroth-Cugell, 1984). One of the guidelines for choosing the cell parameters was to secure a similar range of responses. However, insufficient data prevented obtaining all the parameters from the physiological findings, particularly for parameters of the inverse functions.

The cones' quantum-catches were calculated from a given set of RGB values, using a normalized "standard observer' matrix (in: Wyszecki & Stiles, 1982, p. 612). Each pixel observed was simulated by one cone-triplet ($L$, $M$, $S$ or RGB). Thus, the "center" signal represented the central area of the receptive field of each retinal color-coding cell, simulated by a single cone, as often occurs in the fovea (Lee, 1996). Accordingly, the center size was taken as one pixel, $f_{\mathrm{c}}$ (Eq. (2)). The surround was simulated with an inner radius of 1 pixel and an outer radius of 6 pixels, $f_{\mathrm{s}}$. This simulated surround size was also tested for a smaller radius size of 3 pixels, that corresponded better with the physiological findings (Shapley & Enroth-Cugell, 1984), and yielded the same trend of results. We chose the somewhat larger ratio between the radiuses of the center and surround to avoid boundary "hallow effects" in the images. Electrophysiological findings allowed for a rough estimation of the size and weight function of the "remote" (Creutzfeldt et al., 1991a; Creutzfeldt et al., 1991b; Valberg, Lee, Tigwell, & Creutzfeldt, 1985). Accordingly, we applied "remote" area which was comprised an annulus with an inner and outer radius of 6 and 17 pixels respectively, $f_{\mathrm{r}}$ (Eq. (5)), Fig. 1C. Precise information regarding the size of the remote area (of both first and second adaptation order) is limited. Notwithstanding, the model is not very sensitive to this value. $K_{\mathrm{remote}}$ (Eq. (5)), defined the slope of the weight function, and was taken as the difference between the outer and inner radiuses of the relevant surround and remote areas. This rule was retained for all weight functions across the model, including those of the adaptation of the second order. The first order adaptation parameters (Eq. (9)) were taken as follows: $a_{\mathrm{cen}} = a_{\mathrm{srdn}} = 1$, $b_{\mathrm{cen}} = b_{\mathrm{srdn}} = 1$, $c_{\mathrm{cen}} = c_{\mathrm{srdn}} = 1$. The parameters, which significantly determine the amount of color induction, are $b_{\mathrm{cen}}$, $b_{\mathrm{srdn}}$. A smaller value of each of the b's cause a stronger induction. The same parameter was also found crucial in the color constancy model (Spitzer & Semo, 2002).

The size of the double-opponent receptive field "center", $\mathrm{f_{do\text{-}c}}$, was taken as a single color-coding cell (which its radius is 7 pixels). The surround region, $\mathrm{f_{do\text{-}s}}$, typically had an inner radius of 1 color-coding cell (7 pixels) and an outer radius of 6 color-coding cells (13 pixels), which is in a reasonable physiological range (Conway, Hubel, & Livingstone, 2002). The "remote" region, $f_{\mathrm{r}}$ (Eq. (14)), was taken as an annulus with an inner and outer diameter of 6 and 13 color-coding cells (13 and 24 pixels), respectively. The slope of the weight function, $K_{\mathrm{remote}}$ (Eq. (14)) was determined by the same rule as in the adaptation of the first order. These values fall within the range related to silence regions of the color-coding cells in V1 and V4, (Courtney, Finkel, & Buchsbaum, 1995; Schein & Desimone, 1990). The second-order adaptation parameters (Eq. (24)) were taken as follows: $b_{\mathrm{do}} = 0.3$, $c_{\mathrm{do}} = 1$ and $d_{\mathrm{do}} = 0.3$. The parameter, which significantly determined the amount of contrast induction is $b_{\mathrm{do}}$. A smaller value of $b_{\mathrm{do}}$ causes a stronger contrast induction. A small interaction between the chromatic contrast channels was shown psychophysically (Zaidi et al., 1998). The $d_{\mathrm{do}}$ parameter, determined the strength of the interaction between the different contrast channels (higher value of $d_{\mathrm{do}}$ denotes a higher interaction).

### 3.2. Performance of the model

#### 3.2.1. Psychophysical predictions

*3.2.1.1. Predictions of first-order color adaptation.* Fig. 4 presents examples of the model's predictions for color induction (adaptation of the first order) while different color surroundings were tested on the CIE *XYZ* space. The figure demonstrates the calculated perceived colors in the CIE *xy* chromaticity coordinates, and two examples of induction effect for a green surround and a blue surround (the demonstrations at the left and bottom to the curve figure). The model predictions on the induction effect were performed with two degrees of the model's performance by applying two different values of $b_{cen}$, $b_{srdn}$, to reflect two strengths of the adaptation parameter $\sigma$ (Eqs. (7) and (8)) of the first-order adaptation mechanism ($b_{cen} = b_{srdn} = 1$ and $b_{cen} = b_{srdn} = 0.7$, while preserving all other parameters). The figure demonstrates the model's prediction of the perceived color having a complementary nature. It can be seen (Fig. 4) by the location of the perceived color (colored circles) on the same straight line of the corresponding inducer color (colored star), that crosses the white point in the CIE *xy* chromaticity coordinates (Vos, 1978; Wyszecki & Stiles, 1982). The same complementary prediction was found for surround stimuli which are composed of non-primary colors (i.e., not *L*, *M*, *S* or their complementary colors) as seen in an example in the CIE *xy* chromaticity coordinates (the black dashed line with the *x* symbols).

*3.2.1.2. Predictions of second-order color adaptation.* Figs. 5 and 6 present simulations of two examples of the model's ability to predict the perceived color contrast modulation arising from the surrounding chromatic contrast. The figures demonstrate the dual effect of the model's modulation, surround suppression (Figs. 5A and 6A) and surround enhancement (Figs. 5B and 6B) on the central green and red checkerboard (Fig. 5) and on the central blue and yellow checkerboard (Fig. 6). These predictions are automatically obtained by the model, without changing any of the model's parameters or components. The automatic performance with both dual effect of enhancement and suppression has not been described by previous models (Singer & D'Zmura, 1994; Xing & Heeger, 2001). The right columns demonstrate the modulations of color saturations resulted from the surround contrasts, while the squares patch of each central stimulus is presented in void, before and after the algorithm performance (see the corresponding arrows). The model can also psychophysically predict the color modulation, for textures of non-primary colors, (Singer & D'Zmura, 1994).

For enhanced clarity of the above results (Fig. 5) reflecting the different model stages, we demonstrate below (Figs. 7–10) the intermediate stages of the model and their responses.

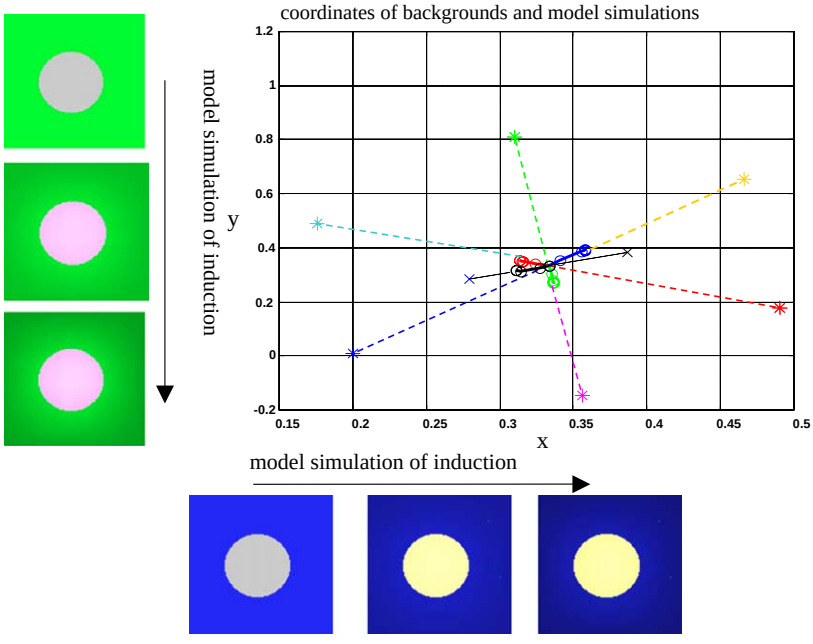


Fig. 4. The model's predictions for different chromatic surrounding stimuli (the colored stars), which cause color induction to the achromatic central stimulus on the CIE *xy* chromaticity coordinates. Note that the colored lines connecting the inducing and the predicted (perceived) color of the central stimuli (the colored circle) cross at the white point and lead to the complementary color for each induced central stimulus. The two sets of images (vertical and horizontal) were simulated at two adaptation strengths, i.e., different values of $b_{cen}$, $b_{srdn}$, in the adaptation of the first order, Eq. (9). The arrows (adjacent to the CIE *xy* chromaticity coordinates) indicate the decrease in the $b_{cen}$, $b_{srdn}$ values (from 1 to 0.7), which causes an increase in the strength of the induction effect (as shown for both color surrounding stimuli).

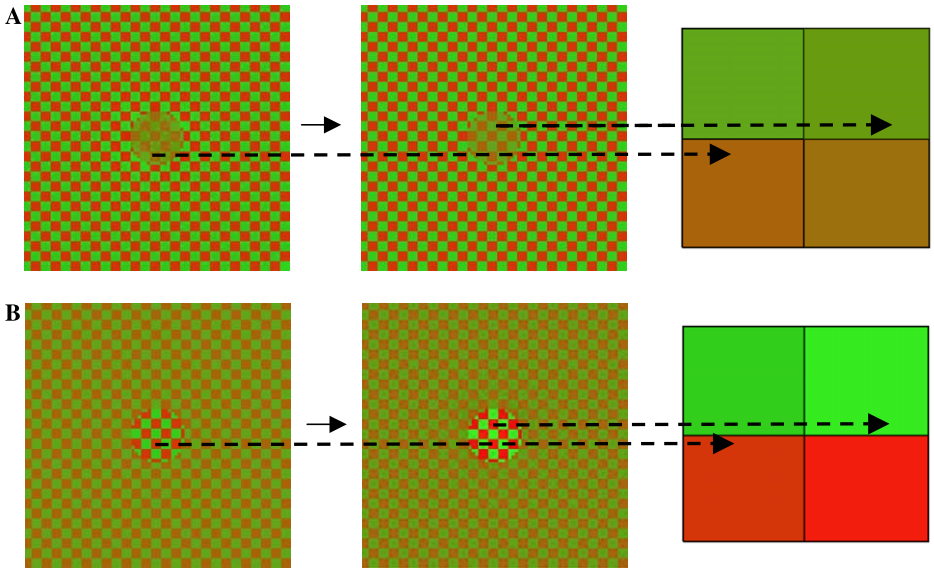


Fig. 5. Demonstration of two examples of the model's prediction for central contrast suppression (A) and enhancement (B) due to the surrounding inducing contrast. The original contrast stimuli are presented in the left column and the model's predictions in the middle column. In order to demonstrate the central contrast chromatic modulation effect due to the surround area, the relevant chromatic squares from the original and predicted central areas are presented in void (right column).

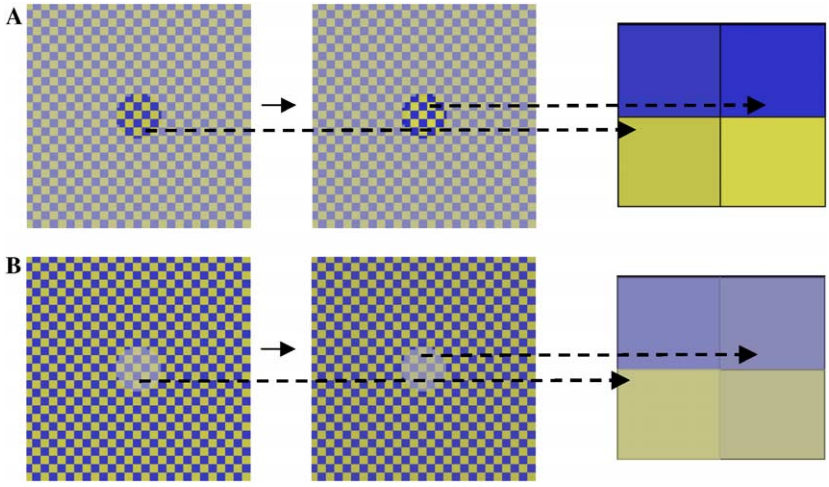


Fig. 6. Demonstration of two examples of the model's prediction with different color composition but with same structure as in Fig. 5.

Fig. 7 illustrates the L/M color-coding cell response ($R_{\mathrm{op}(L^+M^-)}$, Eq. (9)) as an example of color-coding cell responses. As shown in the figure, the response in the central area yields a larger amplitude due to the higher color saturation in the central region. The double opponent stage is illustrated in Fig. 8, as a comparison between the double opponent receptive field responses, $L_{\mathrm{do}}$, and the perceived responses of the double opponent $L'_{\mathrm{do}}$ (in the inverse function calculation, Eq. (24)). At this stage of the model chromatic contrasts are the relevant component therefore absolute values are calculated. The perceived responses of the double opponent yields a higher response in the center area than the response of the double opponent receptive field before the inverse function, due to the adaptation mechanism, which is influenced by the double opponent remote signal (pink line in Fig. 8, Eq. (14)). Note that the psychophysical modulation of the simulated contrast in the central region has a similar trend, and is also expressed similarly to the magnitude of model's modulation response (around 10–20%), which falls in the range of the psychophysical findings (D'Zmura & Singer, 1996; Singer & D'Zmura, 1994). This chromatic enhancement alters the perceived response of the opponent color-coding cell ($R'_{\mathrm{op}(L^+M^-)}$, Eq. (25)) and has a higher amplitude response than the color-coding cell response ($R_{\mathrm{op}(L^+M^-)}$), as demonstrated in Fig. 9.

Fig. 10 presents the model's dual psychophysical prediction of suppressed or enhanced central contrast (D'Zmura & Singer, 1999; Xing & Heeger, 2001). It

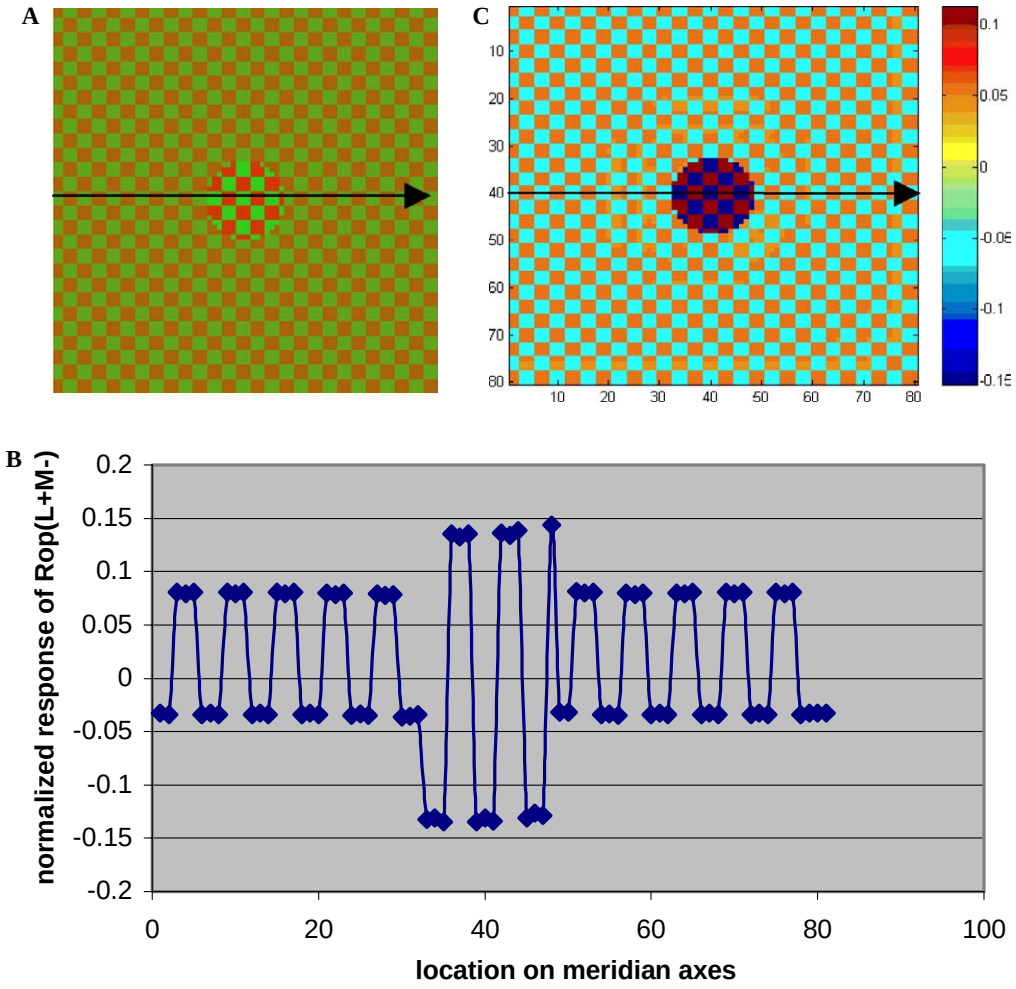


Fig. 7. An illustration of an intermediate stage of the model, of the first order of adaptation, the L/M color-coding cell response ($R_{op(L^+M^-)}$, Eq. (9)) for the stimulus presented in Fig. 5(A). (B) The normalized L/M color-coding cell response, $R_{op(L^+M^-)}$, along the $x$-axis of the stimulus, central bold arrow (A). (C) The cell response is presented as a 2-D image, where the color represents the value of the cell response (according to the color bar).

presents the dependence (Eq. (24)) of the perceived contrast of $L'_{do}$ in this example, as a function of the contrast, $L_{do}$ of this chromatic channel in two different contrast remote areas, 0.4 and 0.7, the red and green curves, respectively. The diagonal 45° dashed black line presents those values where the central and remote contrasts are identical, and therefore yield the same values for the perceived response of the central contrasts, $L'_{do}$. The figure demonstrates that the model predicts both suppression (colored line below the dashed gray line) and enhancement effects (colored line above the dashed gray line), depending on the contrast ratio between the center and the surround areas. These predictions concur with the psychophysical findings (D'Zmura & Singer, 1996; D'Zmura & Singer, 1999; Singer & D'Zmura, 1994).

*3.2.1.3. Effect of textured chromatic surround on the perceived color.* Another recently investigated psychophysical effect of surrounding chromatic variability on a central chromatic patch was tested in this model. A variegated and homogeneous surround were compared and found to have a smaller induction effect, while retaining the same averaged chromaticity and intensity (Brenner & Cornelissen, 2002; Brown & MacLeod, 1997; Shevell & Wei, 1998).

We consider this induction to consist of two types, the first being the chromatic induction of the average color of the surrounding region, and the second, the induction of the surrounding chromatic contrast on the perceived central contrast. Since the first induction (resulting from the average color of the surrounding) causes induction towards the complementary color and is processed first, the second induction (contrast–contrast), which receives its input from the output of the first mechanism, acts on a different contrast channel in the central area, Fig. 11. For example, if the surround is composed of a red and green texture, the first order induction causes induction towards a bluish color (due to the surround average of yellow color). Fig. 11 shows the second order induction acting mainly on single

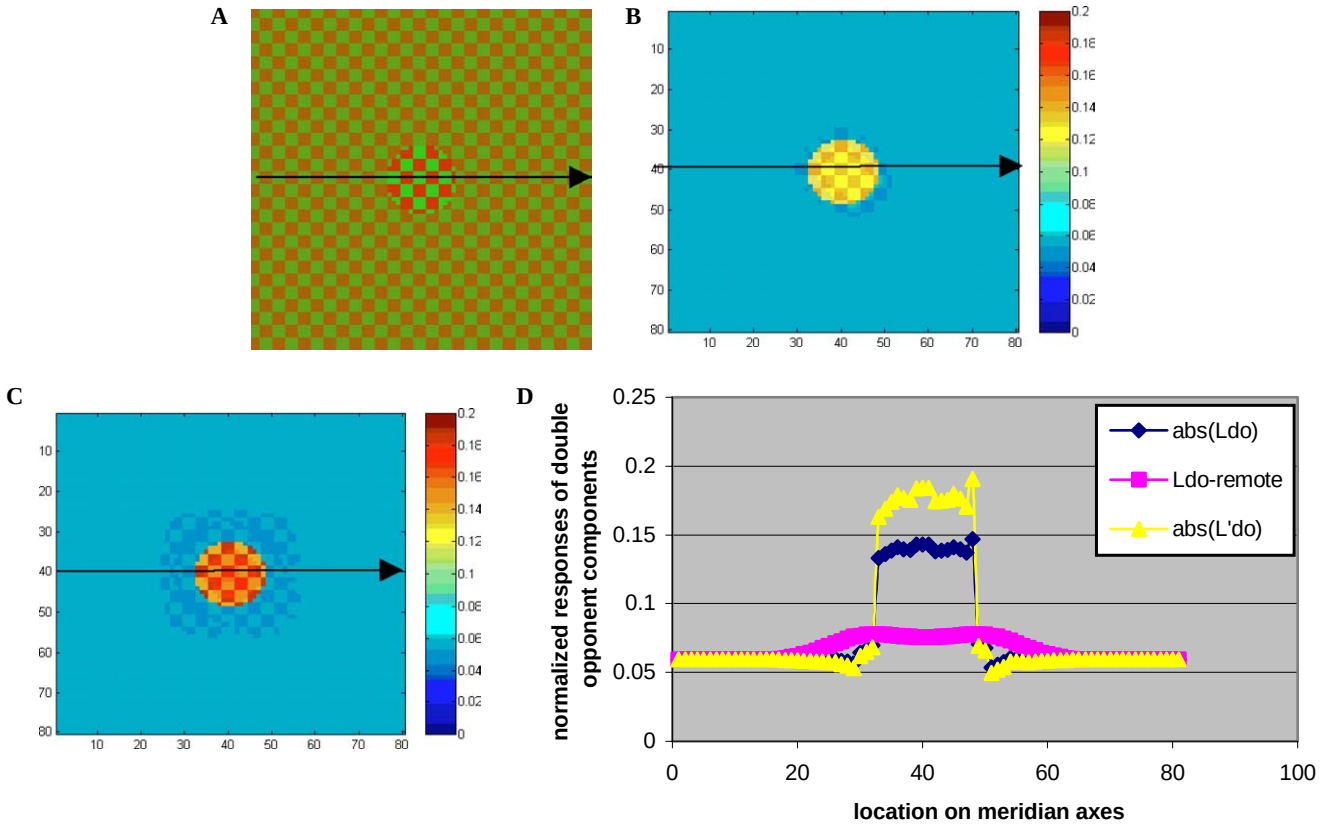


Fig. 8. An illustration of an additional intermediate stage of the model, of the second order of adaptation, to a specific stimulus (A). (B) The absolute response of the double opponent cell before adaptation, $L_{do}$, Eq. (13), is presented as a 2-D image. (C) The perceived absolute $L'_{do}$ response, Eq. (23), is presented as a 2-D image. (D) Responses of different components of the double opponent stage are presented on the same plot as a function of their location across the $x$-axis of the stimulus, central bold arrow (A). The blue line presents the absolute response of $L_{do}$. Note that higher values correspond to the center of the stimulus (A) where the responses have a higher chromatic contrast, as presented in the image (B). To demonstrate the model's performance, the perceived absolute $L'_{do}$ response is presented (Yellow line, Eq. (23)). Note that since the $L_{(do\text{-}remote)}$ (pink line, Eq. (13)) signal is lower than the values of $L_{do}$ in the central area, the $L'_{do}$ response was enhanced in that region.

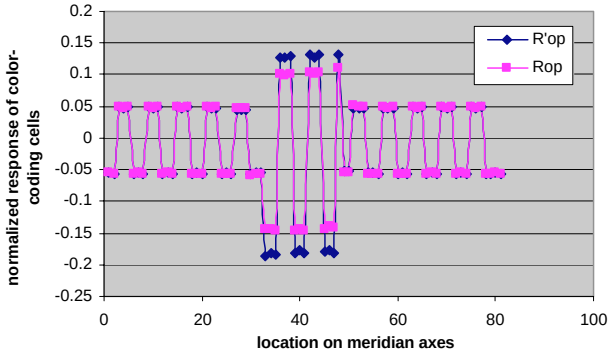


Fig. 9. An illustration of a further intermediate stage of the model, which reflects the inverse function stage. The normalized response of the perceived opponent response $R'_{op(L^+M^-)}$ (blue line, Eq. (25)) is presented as a stage of the inverse function in comparison to the color-coding cell response $R_{op(L^+M^-)}$ (pink line, Eq. (9)).

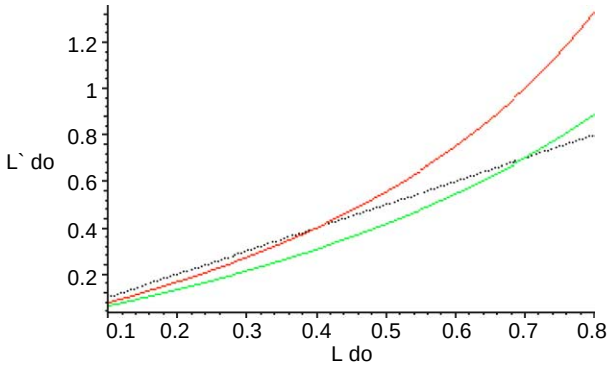


Fig. 10. The model's prediction, $L'_{do}$ Eq. (23), is shown as a function of the color contrast as reflected in the response of the same color channel, $L_{do}$, for two different remote area contrasts 0.4 and 0.7, the red and green curves, respectively, contrasts areas (see text). The figure demonstrates the automatic capability of the model to dual effects of suppression and enhancement (the area below and above the doted gray line).

chromatic contrast channel. The induced contrast is mainly on red-green contrast and not on the induced bluish color.

The suggested model includes a small interaction between the contrast chromatic channels, $d_{do}$ (Eq. (18)), which enables the model to overcome this difficulty and to express more accurately the observed psychophysical results of interaction effect between the

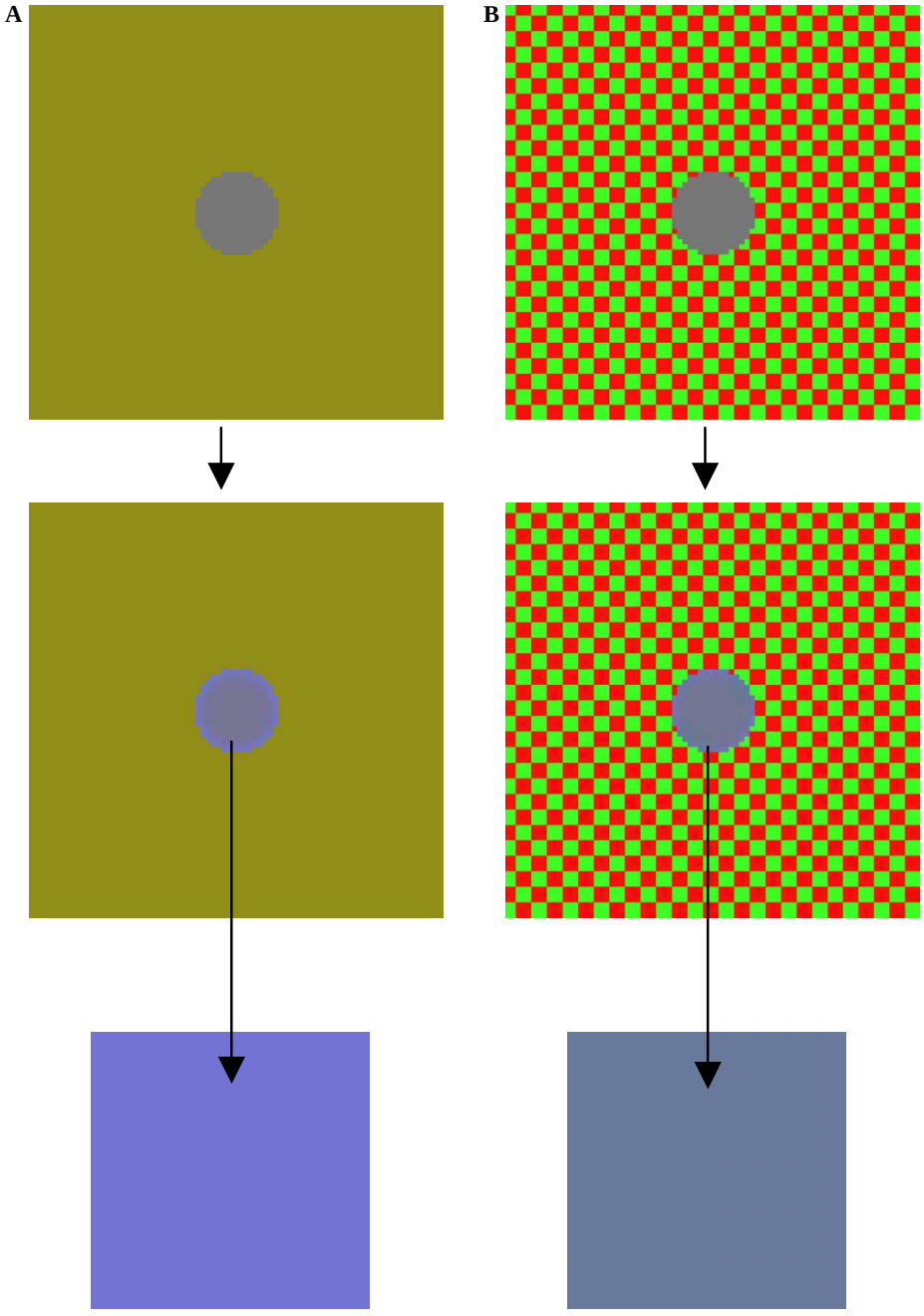


Fig. 11. Demonstration of the model's prediction to yield a smaller induction effect when the surround area is variegated (B), in comparison to the induction effect when the surround area is homogenous (A), even though the average color and intensity are identical in both the input stimuli. The upper row represents the original stimuli, while the second row represents the model's prediction. The lower row represents the induced color (in void) near the center-surround border.

chromatic contrast channels (Brenner & Cornelissen, 2002; Brown & MacLeod, 1997; Shevell & Wei, 1998).

Figs. 11A and B demonstrates the model's induction predictions for homogeneous and variegated surround stimuli, which share the same luminosity and chromaticity (the upper row). Thus, only the chromaticity variability (i.e., contrast) is different. The figure demonstrates the model's prediction (middle row) of obtaining a smaller induction effect for the variegated surround stimuli than the induction for the homogeneous surround.

Fig. 12 demonstrates the model's ability (with the first and the second adaptation orders) to perform simultaneously color constancy and chromatic contrast enhancement on real images, in addition to its ability to predict the different types of induction effects. This ability is demonstrated here on the same set of parameters used for the different chromatic induction effects.

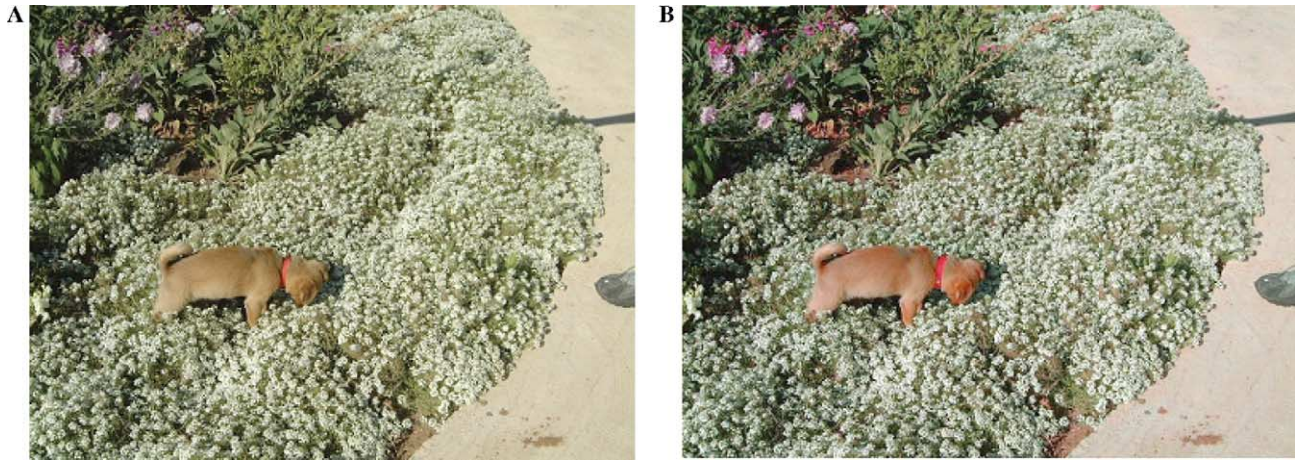


Fig. 12. A demonstration of the suggested physiological model predicting the algorithm's efficiency in different induction effects for applications on real images. The model performs color constancy (the yellowish color on the corrected image has been reduced) and enhancement of color contrast (B) compared to the original image (A). Note the increase in the saturation and chromatic contrast, for example, of the rosy flowers in the left corner of the image (B).

(Our previous applications of the model to two algorithms of color constancy and enhancement of color contrast were performed not necessarily with this exact set of parameters) (Spitzer & Semo, 2002; Spitzer & Sherman, 2002). Fig. 12B shows the color constancy expressed by reducing the yellowish appearance of the original image (A), which derives probably from the chromatic illumination. In addition, the modulation of chromatic contrast can be seen in the enhancement of the rosy colors of the flowers (in left corner of the image (B), on the collar of the dog and greenish colors in addition to enhancement of the details in the image (B).

## 4. Discussion

A computational biological model based on plausible physiological retinal and cortical color-coding receptive fields and physiological adaptation mechanisms of the first and second order is presented, to primarily predict the different types of induction effects. The first part of the model (the adaptation of the first order) successfully predicted the color induction with its complementary color effect, Fig. 4, as well as performed the color constancy on real images, Fig. 12 (Spitzer & Rosenbluth, 2002; Spitzer & Semo, 2002). The second part of the model (the adaptation of the second order), accomplished prediction of the color contrast induction, including the automatic facilitation or inhibition of the perceived contrast, depending on the surrounding contrast, Figs. 5 and 6. The same model can perform color constancy as well as enhance the color contrast on real images, Fig. 12.

The suggested order of color processing, dealing first with the color and then with the color contrast, has an obvious computational advantage. This first order adaptation enables the visual system to first perform perceived color calculations and color constancy, which actually reduce the colored illumination and enhancing the differences of color or/and intensity between different regions. Only then is the second order adaptation performed, the modulation of contrast, in order to enhance the change in color texture and color differences.

### 4.1. Induction effect (Simultaneous contrast)

The model's predictions (adaptation of the first order) show the predictions of the induction effect (Fig. 4), which also leads to complementary perceived colors. Our model anticipated the complementary effect for both the cardinal and non- cardinal colors, as those colors are psychophysically ascertained, and not incorporated in the opponent visual mechanism, (Krauskopf et al., 1986; Semo et al., 1998; Wachtler et al., 2001; Webster & Mollon, 1995). The model's prediction of complementary color by any color induction does not concur with previously suggested computational mechanisms, nor with the suggested neuronal locus of the mechanism proposed by previous studies (Krauskopf et al., 1986; Ware & Cowan, 1987; Zaidi, 1999). The current study contradicts the assumptions of previous studies that assumed that a complementary effect could not be derived from opponent receptive fields type, and therefore could not derive from pre-cortical stages (Brown & MacLeod, 1997; Krauskopf et al., 1986). A previous computational model based on oriented multiscale difference-of-Gaussian (ODOG) filters was suggested for brightness induction and white effect (Blakeslee & McCourt, 1999). Applying this ODOG model to color-coding cells does not predict the color complementary perceived effect.

In addition to the model predictions of color induction effect and its manifestation of complementary effect, the simulated results suggest that the effect of induction of color emanated from the same adaptation mechanism as the effect of color constancy, due to the prediction of both effects by the same part of the model, which can be originated from retinal adaptation mechanisms. This method of the model's prediction also contradicts previous suggestions regarding the origin of induction and color constancy, see also Introduction (Gegenfurtner, 2003; Krauskopf et al., 1986; Wachtler et al., 2003; Zaidi, 1999). Thus, we claim that this assumption of perceived complementary color can be obtained from an adaptation mechanism based on the three most frequently distributed color-coding retinal cells.

Further foundation for the role of cortical mechanism in color constancy arises from the assumption that receptive fields play a role in color constancy and should distinguish between local changes in surface reflectance and global changes in illumination. It has been claimed that the system needs a receptive field that is color opponent in both its center and its surround region to achieve this in the color domain, (Conway et al., 2002; Courtney et al., 1995; Gegenfurtner, 2003; Zeki, 1983). These authors claimed that double opponent receptive fields perform this task while these types of receptive field were found only in the cortical level. We agree that the structure of double opponent receptive fields has the ability to perform such a task, but there is no need for this specific type of cell, since retinal color opponent receptive fields with their adaptation mechanism and remote area (Model) can also fulfill such a task. Furthermore, it is not parsimonious that color constancy would occur in the double opponent receptive field, since the goal of color constancy is to decrease the chromatic illumination which reduces the average color in the scene, while the colors are intermixed twice at the cortical level at the double opponent receptive fields (first in the retinal opponent cells and again in the double opponent cells in V1). Therefore, it would more cost effective for the system using the opponent receptive fields as building blocks, to first process the color information and thereafter using the double opponent receptive fields as building blocks to process the color contrast in the cortical level (second order).

### 4.2. Color contrast induction

The chromatic and the spatial structure of the double opponent cells enable the modulation of chromatic contrast performance, which cannot be performed by color opponent cells (at the first-order adaptation level). This part of the model (second-order adaptation), which successfully predicts psychophysical contrast–contrast effects, was not developed originally only for *ad hoc* prediction of the specific effects of contrast modulations. A variation of the model was also suggested as an algorithm for real chromatic contrast images enhancement (Spitzer & Sherman, 2002).

The spatial and chromatic structure of color cortical receptive fields has been a controversial topic in recent years. It has been found that the majority of V1 cells were luminance- preferring and color luminance cells (Shapley & Hawken, 2002). The color-luminance neuron seems to be elongated rather than circularly symmetric, and many have orientation and spatial frequency selectivity (Johnson, Hawken, & Shapley, 2001; Lennie, 2000; Shapley & Hawken, 2002). These authors found that most of color-preferring cells are of the opponent type and are symmetrical. Contrary to the above, Conway (2001) found that most V1 color cells in alert monkeys were shown to be double opponent also of receptive fields which contain coding of complementary colors (such as red-cyan double opponent receptive fields). The existence of additional chromatic mechanisms (in addition to three common suggested cones) at least at higher levels in the visual pathway has been claimed (see textbook in: Lennie, 2000; Kiper, Fenstemaker, & Gegenfurtner, 1997). For the contrast chromatic induction we chose to use the most suitable plausible color contrast building block, which are the classical double opponent receptive fields (Conway et al., 2002), for this scope of the paper (induction effects). We have not necessarily taken into account all the accumulated electrophysiological findings of cortical color receptive fields with different chromatic structure (Conway, 2001; Shapley & Hawken, 2002). Regarding the percentage of the classical double opponent cells, the literature (Introduction) disputes their potential contribution to specific perceptual performance. We believe they should not be simply excluded, due to their percentage in relation to specific aspect of perception, since there is no simple connection between percentage (not the existence) of specific type of cells in specific cortical area and their role in perception. (We know, for example, that the percentage of the blue receptors is lower than the other chromatic receptors in the retina and still we see the blue color not less than the other colors.) We believe that the other structures of chromatic cortical coding cells are used by the system for visual tasks other than modulation of the chromatic contrast.

Regarding other chromatic contrast induction models, D'Zmura and Singer's model (D'Zmura & Singer, 1999) suggested that the increase in the perceived central color contrast is derived from a reduced gain and channel inhibition. The decrease in perceived central color contrast can be predicted by their model by reversing the sign for one or more channel interaction coefficients in their model. Thus, their psychophysical model, which

is not based on physiological building blocks, does not describe the visual system's automatic performance of this psychophysical dual effect of facilitation and suppression of the central contrast. In our model, this dual effect of perceived enhancement and reduced central contrast due to surround contrast is derived automatically from the same model and parameters (Figs. 5A and B and 6A and B).

A recent work studied the perceived achromatic contrast dependence of center-surround interactions and suggested a computational psychophysical model to account for these spatial contrast interactions (Xing & Heeger, 2001). This extended model with additional components does not enable automatic modulation of the central contrast due to the surround contrast as demonstrated by their psychophysical results. Thus, their model with the same equations does not include both the surround suppression and the surround enhancement of the central contrast effect.

As far as we know, most of the physiological or psychophysical chromatic computational models have not been applied to real images, except for a recent model of D'Zmura & Singer (1999). In this model the algorithm for the contrast gain control equalizes contrast levels across space in real images. Our algorithm performs contrast enhancement (not equalization) (Figs. 10 and 12). D'Zmura and Singer's model (D'Zmura & Singer, 1996; D'Zmura & Singer, 1999; Singer & D'Zmura, 1994) includes luminance induction, which is dependent on experimentally observed spatial frequency. The current suggested version of our model does not include these properties. However, these features are planned to be added in the future.

### *4.3. Effect of textured chromatic surround on the perceived color*

The current model predicts that the induction of the variegated surround causes a smaller effect than the homogeneous color surround (Fig. 11), while the average chromatic and luminance surrounds are identical. This prediction concurs with different psychophysical studies (Brenner & Cornelissen, 2002; Brenner, Ruiz, Herraiz, Cornelissen, & Smeets, 2003; Brown & MacLeod, 1997; Shevell & Wei, 1998; Semo et al., 1998). These studies tested whether the average color of the surround region alone plays a role in the perceived central color, or whether chromatic variability also plays a role. Shevell & Wei (1998) showed that the effect is binocular, and thus supports the suggestion that a cortical locus is responsible for this effect.

In order to predict this type of induction, two types of adaptation, from the first and the second order were necessitated. The first order of adaptation considers only the average color of the surrounding area, and the second order considers the contrast domain of the surround region, but contrast induction is performed mainly on color composition of the surround contrast. Since the first order of adaptation model can cause an induction of perceived complementary color, which is not perfect spatially homogeneous, the second order of adaptation with its interaction factor (Eq. (18)) can cause an effect on the perceived color.

The different effect of the variegated vs. the homogenous surround on the perceived color is relevant in determining or evaluating different color constancy models. Many models have taken the average color of the surrounding areas into account, such as the different Retinex models and recent physiological color constancy models (Land, 1986; Land & McCann, 1971; Spitzer & Rosenbluth, 2002; Spitzer & Semo, 2002). Based on the present model's prediction (Fig. 11), we argue that the findings of the role of the variegated surround on the perceived color do not rule out the color constancy models that rely on the averaged color of the surrounding or remote areas. Accordingly, the first order of color adaptation, or color constancy mechanism, relates to the color domain. At this stage of processing the weighted average chromatic color in the remote areas is the relevant domain, whereas in the second adaptation mechanism, the color contrast is the relevant domain. Since the output of the first order is the input to the second order, the overall perception is reflected by both mechanisms. Consequently, an overall color perception model must also take this effect of surrounding texture into account, as does the current model.

Brenner & Cornelissen (2002) presented a different approach, when they wrote "From a functional perspective we interpret chromatic induction to be a failure of color constancy...". The current model suggests that the color induction and the color constancy mechanism are derived from the same adaptation of the first order mechanism, and that contrast induction which is manifested by textures modulations is derived from color contrast adaptation (adaptation of the second order). In addition, our model endorses the usefulness of induction effects in the visual system for enhancing the differences between objects or surfaces and their surround regions.

We have presented a comprehensive computational physiological model of predictions of different induction effects, whose mechanisms have recently been debated but not modeled in the literature. In conclusion, the predictions of induction effects and the correction and enhancement of real images support the suggested comprehensive physiological model.

## Acknowledgments

We thank David Horn and Solange Akselrod for their useful comments on the manuscript.

## References


Blakeslee, B., & McCourt, M. E. (1999). A multiscale spatial filtering account of the White effect, simultaneous brightness contrast and grating induction. *Vision Res., 39*(26), 4361–4377.

Brenner, E., & Cornelissen, F. W. (2002). The influence of chromatic and achromatic variability on chromatic induction and perceived colour. *Perception, 31*(2), 225–232.

Brenner, E., Ruiz, J. S., Herraiz, E. M., Cornelissen, F. W., & Smeets, J. B. (2003). Chromatic induction and the layout of colours within a complex scene. *Vision Res., 43*(13), 1413–1421.

Brown, R. O., & MacLeod, D. I. (1997). Color appearance depends on the variance of surround colors. *Curr. Biol., 7*(11), 844–849.

Chubb, C., Sperling, G., & Solomon, J. A. (1989). Texture interactions determine perceived contrast. *Proc. Natl. Acad Sci. USA, 86*(23), 9631–9635.

Conway, B. R. (2001). Spatial structure of cone inputs to color cells in alert macaque primary visual cortex (V-1). *J. Neurosci., 21*(8), 2768–2783.

Conway, B. R., Hubel, D. H., & Livingstone, M. S. (2002). Color contrast in macaque V1. *Cereb Cortex., 12*(9), 915–925.

Courtney, S. M., Finkel, L. H., & Buchsbaum, G. (1995). Network simulations of retinal and cortical contributions to color constancy. *Vision Res., 35*(3), 413–434.

Creutzfeldt, O. D., Crook, J. M., Kastner, S., Li, C. Y., & Pei, X. (1991a). The neurophysiological correlates of colour and brightness contrast in lateral geniculate neurons. I. Population analysis. *Exp. Brain Res., 87*(1), 3–21.

Creutzfeldt, O. D., Kastner, S., Pei, X., & Valberg, A. (1991b). The neurophysiological correlates of colour and brightness contrast in lateral geniculate neurons. II. Adaptation and surround effects. *Exp. Brain Res., 87*(1), 22–45.

D'Zmura, M., & Singer, B. (1996). Spatial pooling of contrast in contrast gain control. *J. Opt. Soc. Am. A Opt. Image Sci. Vis., 13*(11), 2135–2140.

D'Zmura, M., & Singer, B. (1999). Contrast gain control. In K. R. G. L. T. Sharpe (Ed.), *Color Vision from genes to perception* (pp. 369–385). Cambridge university press.

Dahari, R., & Spitzer, H. (1996). Spatio-temporal adaptation model for retinal ganglion cells. *Journal of the Optical Society of America A, 13*, 419–439.

De Bonet, J. S., & Zaidi, Q. (1997). Comparison between spatial interactions in perceived contrast and perceived brightness. *Vision Res., 37*(9), 1141–1155.

Fairchild, M. D. (1998). *Color Appearance Models*. (MA): Addison-Wesley.

Gegenfurtner, K. R. (2003). Cortical mechanisms of colour vision. *Nat. Rev. Neurosci., 4*(7), 563–572.

Hayhoe, M. M., & Wenderoth, P. (1991). Adaption mechanisms in color and brightness. In A. Valberg & B. Lee (Eds.), *From pigments to perception* (pp. 353–367). New York: Plenum Press.

Hughes, A., & DeMarco, P. J. (2003). Time course of adaptation to stimuli presented along cardinal lines in color space. *J. Opt. Soc. Am. A. Opt. Image Sci. Vis., 20*(12), 2216–2227.

Johnson, E. N., Hawken, M. J., & Shapley, R. (2001). The spatial transformation of color in the primary visual cortex of the macaque monkey. *Nat. Neurosci., 4*(4), 409–416.

Kaplan, E., & Benardete, E. (2001). The dynamics of primate retinal ganglion cells. *Prog. Brain Res., 134*, 17–34.

Kiper, D. C., Fenstemaker, S. B., & Gegenfurtner, K. R. (1997). Chromatic properties of neurons in macaque area V2. *Vis. Neurosci., 14*(6), 1061–1072.

Krauskopf, J., Zaidi, Q., & Mandler, M. (1986). Mechanisms of simultaneous color induction. *J. Opt. Soc. Am A., 3*(10), 1752–1757.

Land, E. H. (1986). Recent Advances in Retinex Theory. *Vision Res., 26*(1), 7–21.

Land, E. H., & McCann, J. J. (1971). Lightness and retinex theory. *J. Opt. Soc. Am., 61*(1), 1–11.

Lee, B. B. (1996). Receptive field structure in the primate retina. *Vision Res., 36*(5), 631–644.

Lennie, P. (2000). Color Vision. In E. R. Kandel, J. H. Swhartz, & T. M. Jessll (Eds.), *Principles of neuronal science*. McGraw-Hill.

Monnier, P., & Shevell, S. K. (2003). Large shifts in color appearance from patterned chromatic backgrounds. *Nat. Neurosci., 6*(8), 801–802.

Rinner, O., & Gegenfurtner, K. R. (2000). Time course of chromatic adaptation for color appearance and discrimination. *Vision Res., 40*(14), 1813–1826.

Sakmann, B., & Creutzfeldt, O. D. (1969). Scotopic and mesopic light adaptation in the cat's retina. *Pflugers Archiv., 313*, 168–185.

Schein, S. J., & Desimone, R. (1990). Spectral properties of V4 neurons in the macaque. *J. Neurosci., 10*(10), 3369–3389.

Semo, S., Rosenbluth, A., Spitzer, H., 1998. Remote adaptation in colour vision–experimental study. ECVP '98 (Perception).

Shapiro, A. G., Beere, J. L., & Zaidi, Q. (2003). Time-course of S-cone system adaptation to simple and complex fields. *Vision Res., 43*(10), 1135–1147.

Shapley, R., & Enroth-Cugell, C. (1984). Visual Adaptation and Retinal Gain Controls. *Progress in retinal Research, 3*, 263–346.

Shapley, R., & Hawken, M. (2002). Neural mechanisms for color perception in the primary visual cortex. *Curr. Opin. Neurobiol., 12*(4), 426–432.

Shevell, S. K., & Wei, J. (1998). Chromatic induction: Border contrast or adaptation to surrounding light? *Vision Res., 38*(11), 1561–1566.

Shevell, S. K., & Wei, J. (2000). A central mechanism of chromatic contrast. *Vision Res., 40*(23), 3173–3180.

Singer, B., & D'Zmura, M. (1994). Color contrast induction. *Vision Res., 34*(23), 3111–3126.

Solomon, S. G., Peirce, J. W., & Lennie, P. (2004). The impact of suppressive surrounds on chromatic properties of cortical neurons. *J. Neurosci., 24*(1), 148–160.

Spitzer, H., & Hochstein, S. (1985). A complex-cell receptive-field model. *J. Neurophysiol., 53*(5), 1266–1286.

Spitzer, H., & Rosenbluth, A. (2002). Color constancy: The role of low-level mechanisms. *Spatial Vision, 15*, 277–302.

Spitzer, H., & Semo, S. (2002). Color constancy: A biological model and its application for still and video images. *Pattern Recognition, 35*, 1645–1659.

Spitzer, H., Sherman, E., 2002. Color Contrast: A Biological Model and its Application for Real Images. The First European Conference on Color in Graphics, Imaging and Vision (CGIV) (Poitiers, France).

Ts'o, D. Y., & Gilbert, C. D. (1988). The organization of chromatic and spatial interactions in the primate striate cortex. *J. Neurosci., 8*(5), 1712–1727.

Valberg, A., Lee, B. B., Tigwell, D. A., & Creutzfeldt, O. D. (1985). A simultaneous contrast effect of steady remote surrounds on responses of cells in macaque lateral geniculate nucleus. *Exp. Brain Res., 58*(3), 604–608.

Vos, J. J. (1978). Colorimetric and photometric properties of a 2-deg fundamental observer. *Color Research and Application, 3*, 125–128.

Wachtler, T., Albright, T. D., & Sejnowski, T. J. (2001). Nonlocal interactions in color perception: Nonlinear processing of chromatic signals from remote inducers. *Vision Res., 41*(12), 1535–1546.

Wachtler, T., Sejnowski, T. J., & Albright, T. D. (2003). Representation of color stimuli in awake macaque primary visual cortex. *Neuron, 37*(4), 681–691.

Ware, C., & Cowan, W. B. (1987). Chromatic Mach bands: Behavioural evidence for lateral inhibition in human color vision. *Perception and Psychophysics, 41*, 173–178.

Webster, M. A., & Mollon, J. D. (1995). Colour constancy influenced by contrast adaptation. *Nature, 373*(6516), 694–698.

Wyszecki, G., & Stiles, W. S. (1982). *Color Science: Concepts and Methods, Quantitative Data and Formulae*. John Wiley & Sons.

Xing, J., & Heeger, D. J. (2001). Measurement and modeling of center-surround suppression and enhancement. *Vision Res., 41*(5), 571–583.

Zaidi, Q., Spehar, B., & DeBonet, J. (1998). Adaptation to textured chromatic fields. *J. Opt. Soc. Am A. Opt. Image Sci. Vis., 15*(1), 23–32.

Zaidi, Q. C. (1999). Color and brightness induction: From Mach bands to three-dimensional configurations. In K. R. Gegenfurtner & L. T. Sharpe (Eds.), *Color Vision from gens to perception* (pp. 317–343). Cambridge University Press.

Zeki, S. (1983). Colour coding in the cerebral cortex: The reaction of cells in monkey visual cortex to wavelengths and colours. *Neuroscience, 9*(4), 741–765.